JOURNAL OF COMPUTATIONAL PHYSICS 1, 367–381 (1967)

# Numerical Solution of Plane Viscous Shock Reflections

TZU-SIEN SHAO[1]

*Bell Telephone Laboratories, Incorporated*

*Murray Hill, New Jersey*

## ABSTRACT

A numerical method is presented for solving two-dimensional viscous fluid flow problems. Emphasis is placed on the formulation and solution of weak shock reflections. Time-dependent Newtonian conservation equations are used without heat conduction. They are numerically integrated by a stable difference scheme to obtain asymptotically stationary solutions. Independent variables are transformed to reduce computation time. Numerical results are given for asymptotically stationary weak shock reflections. Reflected shock angles for both regular and Mach reflections obtained agree well with those given by shock-tube experiments.

## I. INTRODUCTION

When a plane shock strikes a smooth rigid wall with small angle of incidence, it gives rise to a regular (two-shock) reflection as shown in Fig. 1. For large angle of incidence, an irregular and more complex type of reflection appears, known as the Mach (three-shock) reflection (Fig. 1).

Von Neumann's [1] two-shock theory works well for simple shock problems and agrees with Smith's [2] experiments. Many authors [3]–[6] have numerically solved stationary shock-flow problems with artificial viscosity and no heat con-

[1] This work was supported by the Atomic Energy Commission under Contract US AEC AT(11-1)1469 and by the National Science Foundation under Contract NSF-GP-4636. It is a part of the thesis submitted in partial fulfillment of the requirements for the degree of Doctor of Philosophy in Mathematics in the Graduate College of the University of Illinois.

duction. Due to numerical difficulties, some of them [3]–[5] have integrated time-dependent equations describing the flow to obtain asymptotically stationary solution. Their results agree quite well with experimental data for simple shock problems and two-shock reflections.

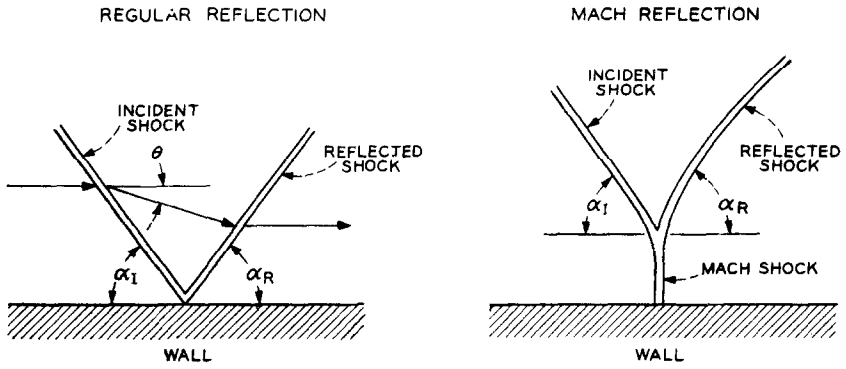


FIG. 1. Regular and Mach Reflections

Unfortunately, for Mach reflections, no method seems to work. In particular, Von Neumann's three-shock theory and various other numerical methods fail badly for Mach reflections with weak incident shocks. There is a wide discrepancy between the predicted shock-reflection angles and Smith's shock-tube experimental results.

Von Neumann's theory used Rankine–Hugoniot equations locally in the neighborhood of the shock-intersection point. It did not work for weak Mach reflections presumably because the viscosity and downstream flow field were ignored. These small effects may be more significant when the incident shock becomes weak. Numerical methods failed presumably for the same reason.

Our method for numerical solution of shock-reflection problems will be as follows. We shall proceed to numerically integrate the time-dependent differential equations on the assumption that the true viscosity terms should be retained. Because weak shocks are to be investigated, it is reasonable to assume that the viscosity coefficient is constant and also that the heat conduction terms can be neglected.

In Section II, Newtonian conservation equations will be written in Lagrangian form. The time-dependent, non heat-conductive partial differential equations will be transformed into a streamline-like coordinate system in Section III. Numerical solution of two-dimensional viscous shock reflection problems together with stability condition will be given in Section IV. The basic numerical procedure is,

fashioned after the PIC method [5], to interpolate the flow variables at the fixed Eulerian mesh points after each Lagrangian time cycle. A graph consisting of data obtained from Von Neumann's theory and our numerical solutions as compared to experiments will be given. Good agreement for weak shock reflections between our results and Smith's experimental data will be demonstrated.

## II. Differential Equations in Lagrangian Form

The theory of fluid flow that we will use is based on the Newtonian mechanics of a small body. In the following, we shall use a dot over a function to denote the Euler's rule of differentiation:

$$\dot{\cdot} = \frac{\partial}{\partial t} + u_1 \frac{\partial}{\partial x_1} + u_2 \frac{\partial}{\partial x_2} = \frac{\partial}{\partial t} + u_i \frac{\partial}{\partial x_i}, \qquad i = 1, 2,$$

and the summation convention. Furthermore, the notation of a comma followed by a subscript $i$ means partial derivatives of functions with respect to $x_i$. Using the assumptions made earlier, the time-dependent, two-dimensional, viscous equations in Lagrangian form [7] can now be written as follows:

(1) Continuity Equation

$$\dot{\varrho} + \varrho u_{i,i} = 0, \qquad i = 1, 2; \tag{2.1}$$

(2) Momentum Equations

$$\varrho \dot{u}_i = [\mu(u_{i,j} + u_{j,i}) - \tfrac{2}{3}\mu u_{k,k}\delta_{ij} - p\delta_{ij}]_{,j} \qquad j = 1, 2, \tag{2.2}$$

where $\mu$ is the coefficient of viscosity and $\delta_{ij}$ is the Kronecker delta;

(3) Energy Equation

$$[\varrho(e + \tfrac{1}{2}u_i u_i)]^{\cdot} = [\mu u_j(u_{i,j} + u_{j,i}) - \tfrac{2}{3}\mu u_{k,k}u_i - pu_i]_{,i} - \varrho(e + \tfrac{1}{2}u_i u_i)u_{j,j} \tag{2.3}$$

where $e$ is the specific internal energy.

The fifth equation is simply the equation of state,

$$p = (\gamma - 1)\varrho e, \tag{2.4}$$

where $\gamma$ is the ratio of specific heats.

## III. Equations in Streamline-Like Coordinate System

For stationary and pseudo-stationary flows, Taub [8] introduced a pair of independent variables, $s$ and $y$. For fixed time $t$, the curves $s =$ constant are the streamlines of particles which have crossed a given curve, say $y = 0$, at times earlier than $t$ and $y$ represents the arc length that a particle has traveled along the curve $s =$ constant, measured from $y = 0$. Since the family of streamlines carries most of the flow information, it is natural to use the streamlines as one of the fundamental coordinates in computation.

In addition to the natural reason of using these coordinates, there are numerical advantages. The Eulerian "interpolation" formulas used after each Lagrangian time cycle will be simpler in this case. Also simplification of boundary conditions can save computation time quite appreciably.

For time-dependent problems, the streamlines vary in time. This gives rise to a delicate question as to whether or not they can be used to define coordinates. Since we are dealing with asymptotically stationary problems, we propose to ignore the movements of streamlines in time. We shall still use the coordinates $(s, y)$ defined by Taub in our numerical method. They will be referred to as the streamline-like coordinates, although streamlines do not exist in time-dependent problems in the strictest sense.

Now let $v^2 = u_i u_i$ be the magnitude of the velocity vector and $(\beta + \frac{1}{2}\pi)$ be the inclination of the curves $s =$ constant in the $(x_1, x_2)$-plane. Furthermore, let us introduce $\eta$ and $\zeta$ to be the parameters associated with the geometry of the coordinate system [9]. Using the differential identities given in [8] and differential relations needed for viscosity terms [9], we can transform the Eqs. (2.1)–(2.3) into the new coordinate system and obtain [9]

(1) Continuity Equation

$$\dot{\varrho} = -\varrho\psi; \tag{3.1}$$

(2) Momentum Equations

$$\varrho\dot{v} = \frac{\mu}{\eta}\left(\frac{\partial\varphi}{\partial s} - \zeta\frac{\partial\varphi}{\partial y}\right) + \frac{4}{3}\mu\frac{\partial\psi}{\partial y} - \frac{\partial p}{\partial y}, \tag{3.2}$$

$$\varrho v\dot{\beta} = \frac{4}{3}\frac{\mu}{\eta}\left(\frac{\partial\psi}{\partial s} - \zeta\frac{\partial\psi}{\partial y}\right) - \mu\frac{\partial\varphi}{\partial y} + \frac{\zeta}{\eta}\frac{\partial p}{\partial y} - \frac{1}{\eta}\frac{\partial p}{\partial s}; \tag{3.3}$$

and

(3) Energy Equation

$$\dot{p} = \mu(\gamma - 1)\left[\frac{4}{3}\psi^2 + \varphi^2 + 4v\left(\frac{\partial\beta}{\partial y}\frac{\partial v}{\partial s} - \frac{\partial\beta}{\partial s}\frac{\partial v}{\partial y}\right)\right] - \gamma p\psi, \tag{3.4}$$

where

$$\psi = \frac{v}{\eta}\left(\frac{\partial \beta}{\partial s} - \zeta \frac{\partial \beta}{\partial y}\right) + \frac{\partial v}{\partial y}; \tag{3.5}$$

$$\varphi = \frac{1}{\eta}\left(\frac{\partial v}{\partial s} - \zeta \frac{\partial v}{\partial y}\right) - v \frac{\partial \beta}{\partial y}, \tag{3.6}$$

and we have used Eq. (2.4) to obtain Eq. (3.4).

The differential equations for $\eta$ and $\zeta$ are simply

$$\frac{\partial \eta}{\partial y} = \frac{\partial \beta}{\partial s} - \zeta \frac{\partial \beta}{\partial y}, \tag{3.7}$$

$$\frac{\partial \zeta}{\partial y} = \eta \frac{\partial \beta}{\partial y}. \tag{3.8}$$

Now, Eqs. (3.1)–(3.8) form a set of eight first-order nonlinear partial differential equations in eight unknowns $\varrho$, $v$, $\beta$, $p$, $\varphi$, $\psi$, $\eta$, and $\zeta$. They describe the two-dimensional viscous fluid flow phenomena in streamline-like coordinates when appropriate boundary conditions are specified.

## IV. Numerical Solution of Regular and Mach Reflections

In this section, we shall describe a numerical procedure of solving shock-reflection problems. Detailed stability analysis of the procedure is given in [9]. To simplify the computation, we consider a two-dimensional rectangular box (Fig. 2) where uniform fluid comes in from the left and exits continuously at the right. The top and bottom boundaries are assumed rigid and smooth. The boundary-layer effects will be ignored completely.

One way of generating a steady incident shock in the flow is to place a straight half-wedge with angle $\omega$ on the bottom boundary of the box. Flow will then be disturbed starting at the tip of the wedge. If the incoming flow is supersonic and the wedge angle is small, a fairly straight attached shock will appear as shown in Fig. 2. Using this simple arrangement, desired incident shock angle $\alpha_I$ and its strength (the pressure ratio across the shock) $\xi_I$ can easily be achieved by fixing the half-wedge angle $\omega$ and the incoming-flow Mach number.

In the present calculations, a square mesh of $50 \times 25$ is set up in the rectangular box in streamline-like coordinates. The standard second-order finite-difference equations derivable from Eqs. (3.1)–(3.4) are applied at each mesh point

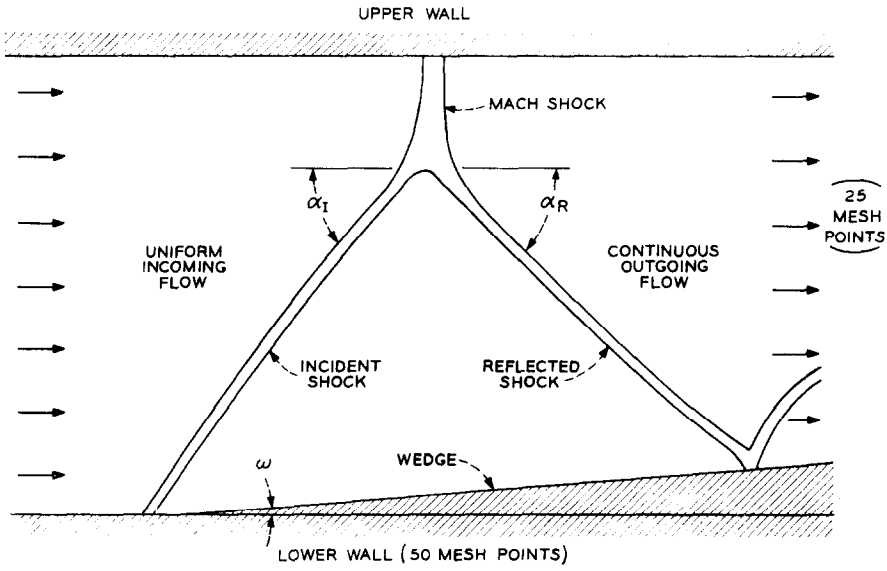


FIG. 2. Two-dimensional shock-reflection configuration.

with uniform time-step $\Delta t$ and space-step $\Delta h$. (Throughout this section, we shall use, for each variable, the superscript $n$ to denote the $n$th time-step and the subscripts $l$ and $m$ to denote the $l$th mesh point on the $m$th streamline.) They can be written in the following form:

$$\bar{\varrho}^{n+1}_{l,m} = \varrho^n_{l,m} - \Delta t \varrho^n_{l,m} \psi^n_{l,m}, \tag{4.1}$$

$$\bar{v}^{n+1}_{l,m} = v^n_{l,m} + \frac{\Delta t}{\varrho^n_{l,m}} \left[ \frac{\mu}{\eta^n_{l,m}} \left( \frac{\varphi^n_{l,m+1/2} - \varphi^n_{l,m-1/2}}{\Delta h} - \zeta^n_{l,m} \frac{\varphi^n_{l+1/2,m} - \varphi^n_{l-1/2,m}}{\Delta h} \right) \right.$$

$$\left. + \frac{4}{3} \mu \frac{\psi^n_{l+1/2,m} - \psi^n_{l-1/2,m}}{\Delta h} - \frac{p^n_{l+1,m} - p^n_{l-1,m}}{2\Delta h} \right], \tag{4.2}$$

$$\bar{\beta}^{n+1}_{l,m} = \beta^n_{l,m} + \frac{\Delta t}{\varrho^n_{l,m} v^n_{l,m}} \left[ \frac{\frac{4}{3}\mu}{\eta^n_{l,m}} \left( \frac{\psi^n_{l,m+1/2} - \psi^n_{l,m-1/2}}{\Delta h} - \zeta^n_{l,m} \frac{\psi^n_{l+1/2,m} - \psi^n_{l-1/2,m}}{\Delta h} \right) \right.$$

$$\left. - \mu \frac{\varphi^n_{l+1/2,m} - \varphi^n_{l-1/2,m}}{\Delta h} + \frac{\zeta^n_{l,m}}{\eta^n_{l,m}} \frac{p^n_{l+1,m} - p^n_{l-1,m}}{2\Delta h} - \frac{1}{\eta^n_{l,m}} \frac{p^n_{l,m+1} - p^n_{l,m-1}}{2\Delta h} \right], \tag{4.3}$$

and

$$\bar{p}^{n+1}_{l,m} = p^n_{l,m} + \Delta t \left\{ \mu(\gamma - 1) \left[ \frac{4}{3} (\psi^n_{l,m})^2 + (\varphi^n_{l,m})^2 + 4 v^n_{l,m} \left( \frac{\beta^n_{l+1,m} - \beta^n_{l-1,m}}{2\Delta h} \right. \right. \right.$$

$$\left. \left. \left. \frac{v^n_{l,m+1} - v^n_{l,m-1}}{2\Delta h} - \frac{\beta^n_{l,m+1} - \beta^n_{l,m-1}}{2\Delta h} \frac{v^n_{l+1,m} - v^n_{l-1,m}}{2\Delta h} \right) \right] - \gamma p^n_{l,m} \psi^n_{l,m} \right\}. \tag{4.4}$$

In order to keep uniform error in the difference equations, we use half-mesh values of $\varphi$ and $\psi$ in the corresponding difference quotients. These half-mesh values can be computed from Eqs. (3.5)–(3.6) as follows:

$$\psi^{\eta}_{l+1/2,m} = \frac{\nu^{\eta}_{l+1/2,m}}{\eta^{\eta}_{l+1/2,m}} [(\beta_s)^{\eta}_{l+1/2,m} - \zeta^{\eta}_{l+1/2,m}(\beta_y)^{\eta}_{l+1/2,m}] + \frac{\nu^{\eta}_{l+1,m} - \nu^{\eta}_{l,m}}{\Delta h} \tag{4.5}$$

and

$$\psi^{\eta}_{l,m+1/2} = \frac{\nu^{\eta}_{l,m+1/2}}{\eta^{\eta}_{l,m+1/2}} [(\beta_s)^{\eta}_{l,m+1/2} - \zeta^{\eta}_{l,m+1/2}(\beta_y)^{\eta}_{l,m+1/2}] + \frac{\nu^{\eta}_{l,m+1} - \nu^{\eta}_{l,m}}{\Delta h}, \tag{4.6}$$

where

$$\nu^{\eta}_{l+1/2,m} = \tfrac{1}{2}(\nu^{\eta}_{l+1,m} + \nu^{\eta}_{l,m}), \tag{4.7}$$

$$\nu^{\eta}_{l,m+1/2} = \tfrac{1}{2}(\nu^{\eta}_{l,m+1} + \nu^{\eta}_{l,m}), \tag{4.8}$$

$$(\beta_s)^{\eta}_{l+1/2,m} = \frac{\beta^{\eta}_{l+1/2,m+1} - \beta^{\eta}_{l+1/2,m-1}}{2\Delta h} = \frac{\beta^{\eta}_{l+1,m+1} + \beta^{\eta}_{l,m+1} - \beta^{\eta}_{l+1,m-1} - \beta^{\eta}_{l,m-1}}{4\Delta h}, \tag{4.9}$$

$$(\beta_s)^{\eta}_{l,m+1/2} = \frac{\beta^{\eta}_{l,m+1} - \beta^{\eta}_{l,m}}{\Delta h}. \tag{4.10}$$

$$(\beta_y)^{\eta}_{l+1/2,m} = \frac{\beta^{\eta}_{l+1,m} - \beta^{\eta}_{l,m}}{\Delta h}, \tag{4.11}$$

and

$$(\beta_y)^{\eta}_{l,m+1/2} = \frac{\beta^{\eta}_{l+1,m+1/2} - \beta^{\eta}_{l-1,m+1/2}}{2\Delta h} = \frac{\beta^{\eta}_{l+1,m+1} + \beta^{\eta}_{l+1,m} - \beta^{\eta}_{l-1,m+1} - \beta^{\eta}_{l-1,m}}{4\Delta h}. \tag{4.12}$$

Since $\psi^{\eta}_{l-1/2,m}$ and $\psi^{\eta}_{l,m-1/2}$ are already available from previous calculations, we have

$$\psi^{\eta}_{l,m} = \tfrac{1}{4}(\psi^{\eta}_{l+1/2,m} + \psi^{\eta}_{l-1/2,m} + \psi^{\eta}_{l,m+1/2} + \psi^{\eta}_{l,m-1/2}). \tag{4.13}$$

Similar expressions for half-mesh values of $\varphi$ can also be derived. As for the half-mesh and mesh-point values of $\eta$ and $\zeta$, we numerically integrate Eqs. (3.7)–(3.8) along $s$ = constant and get two simultaneous equations in $\eta^{\eta}_{l+1/2,m}$ and $\zeta^{\eta}_{l+1/2,m}$:

$$\eta^{\eta}_{l+1/2,m} + \frac{\Delta h}{2}(\beta_y)^{\eta}_{l,m}\zeta^{\eta}_{l+1/2,m} = \eta^{\eta}_{l-1/2,m} - \Delta h(\beta_s)^{\eta}_{l,m} - \frac{\Delta h}{2}\zeta^{\eta}_{l-1/2,m}(\beta_y)^{\eta}_{l,m}, \tag{4.14}$$

and

$$-\frac{\Delta h}{2}(\beta_y)^n_{l,m}\eta^n_{l+1/2,m}+\zeta^n_{l+1/2,m}=\zeta^n_{l-1/2,m}+\frac{\Delta h}{2}\eta^n_{l-1/2,m}(\beta_y)^n_{l,m}. \tag{4.15}$$

With the values of $\eta^n_{l-1/2,m}$ and $\zeta^n_{l-1/2,m}$ given by previous calculations, the solution of Eqs. (4.10)–(4.11) can be written

$$\eta^n_{l+1/2,m}=\frac{\{1-[\frac{1}{2}(\Delta h)(\beta_y)^n_{l,m}]^2\}\eta^n_{l-1/2,m}-\Delta h(\beta_y)^n_{l,m}\zeta_{l-1/2,m}+\Delta h(\beta_s)^n_{l,m}}{1+[\frac{1}{2}(\Delta h)(\beta_y)^n_{l,m}]^2} \tag{4.16}$$

and

$$\zeta^n_{l+1/2,m}=\frac{\Delta h(\beta_y)^n_{l,m}\eta^n_{l-1/2,m}+\{1-[\frac{1}{2}(\Delta h)(\beta_y)^n_{l,m}]^2\}\zeta^n_{l-1/2,m}+\frac{1}{2}(\Delta h^2)(\beta_y)^n_{l,m}(\beta_s)^n_{l,m}}{1+[\frac{1}{2}(\Delta h)(\beta_y)^n_{l,m}]^2} \tag{4.17}$$

where

$$(\beta_y)^n_{l,m}=\frac{\beta^n_{l+1,m}-\beta^n_{l-1,m}}{2\Delta h} \tag{4.18}$$

and

$$(\beta_s)^n_{l,m}=\frac{\beta^n_{l,m+1}-\beta^n_{l,m-1}}{2\Delta h}. \tag{4.19}$$

We also have

$$\eta^n_{l,m}=\tfrac{1}{2}(\eta^n_{l+1/2,m}+\eta^n_{l-1/2,m}), \tag{4.20}$$

and

$$\zeta^n_{l,m}=\tfrac{1}{2}(\zeta^n_{l+1/2,m}+\zeta^n_{l-1/2,m}). \tag{4.21}$$

Slightly more complicated expressions for $\eta^n_{l,m+1/2}$ and $\zeta^n_{l,m+1/2}$ can be derived by using the same method.

Since $\bar{\varrho}^{n+1}_{l,m}$, $\bar{v}^{n+1}_{l,m}$, $\bar{\beta}^{n+1}_{l,m}$, and $\bar{p}^{n+1}_{l,m}$ are the intermediate flow variables of the $l$th mesh point on the $m$th streamline at the $(n+1)$-time cycle, we need perform the interpolation process to combine them with the values of appropriate neighboring mesh point. The transport effect of each variable for asymptotically steady flow can thus be obtained. In our coordinates, this process is very simple. Since the mesh points are all moving unidirectionally from left to right along curves $s=$ constant in the shock-reflection problem, it is only necessary to consider the following case. For fixed $m$ and $v^n_{l,m}\geq 0$, the weighted linear interpolation for $\varrho^{n+1}_{l,m}$, $v^{n+1}_{l,m}$, $\beta^{n+1}_{l,m}$, and $p^{n+1}_{l,m}$ are performed according to the formulas

$$\varrho^{n+1}_{l,m}=A\bar{\varrho}^{n+1}_{l-1,m}+B\bar{\varrho}^{n+1}_{l,m}, \tag{4.22}$$

$$v^{n+1}_{l,m}=A\bar{v}^{n+1}_{l-1,m}+B\bar{v}^{n+1}_{l,m}, \tag{4.23}$$

$$\beta^{n+1}_{l,m}=A\bar{\beta}^{n+1}_{l-1,m}+B\bar{\beta}^{n+1}_{l,m}, \tag{4.24}$$

and

$$p^{\eta+1}_{l,m} = A\bar{p}^{\eta+1}_{l-1,m} + B\bar{p}^{\eta+1}_{l,m}, \tag{4.25}$$

where

$$A = \frac{v^{\eta}_{l,m}\Delta t}{\Delta h - v^{\eta}_{l-1,m}\Delta t + v^{\eta}_{l,m}\Delta t}, \tag{4.26}$$

and

$$B = \frac{\Delta h - v^{\eta}_{l-1,m}\Delta t}{\Delta h - v^{\eta}_{l-1,m}\Delta t + v^{\eta}_{l,m}\Delta t}. \tag{4.27}$$

The set of Equations (4.1)–(4.27) completely describes the numerical iteration procedure for two-dimensional viscous shock-reflection problems. The boundary conditions for the problem shown in Fig. 2 are thanks to our coordinate system, simply as follows.

(1) Left side (uniform incoming flow)

$$\varrho^{n}_{2,m} = \varrho^{n}_{1,m}, \quad v^{n}_{2,m} = v^{n}_{1,m}, \quad \beta^{n}_{2,m} = \beta^{n}_{1,m}, \quad p^{n}_{2,m} = p^{n}_{1,m},$$
$$\psi^{n}_{1/2,m} = 0, \quad \varphi^{n}_{1/2,m} = 0 \quad \text{for} \quad m = 1, 2, \ldots, M;$$

(2) Right side (continuous outgoing flow)

$$\varrho^{n}_{L,m} = \varrho^{n}_{L-1,m}, \quad v^{n}_{L,m} = v^{n}_{L-1,m}, \quad \beta^{n}_{L,m} = \beta^{n}_{L-1,m},$$
$$p^{n}_{L,m} = p^{n}_{L-1,m} \quad \text{for} \quad m = 1, 2, \ldots, M;$$

(3) Top side (rigid smooth wall)

$$\varrho^{\eta}_{l,M} = \varrho^{\eta}_{l,M-1}, \quad v^{\eta}_{l,M} = v^{\eta}_{l,M-1}, \quad \beta^{\eta}_{l,M} = \pi - \beta^{\eta}_{l,M-1},$$
$$p^{\eta}_{l,M} = p^{\eta}_{l,M-1} \quad \text{for} \quad l = 1, 2, \ldots, L;$$

(4) Bottom side (rigid smooth wall with straight wedge)

$$\varrho^{\eta}_{l,1} = \varrho^{\eta}_{l,2}, \quad v^{\eta}_{l,1} = v^{\eta}_{l,2}, \quad \beta^{\eta}_{l,1} = \pi - \beta^{\eta}_{l,2},$$
$$\varrho^{\eta}_{l,1} = p^{\eta}_{l,2} \quad \text{for} \quad l = 1, 2, \ldots, L;$$

an

$$\beta^{\eta}_{l,1} = \pi + 2\omega - \beta^{\eta}_{l,2}$$

for mesh points where the wedge lies.

The angle $\pi$ appears in above conditions because we want to maintain zero

velocity component normal to the walls. In actual computation, the starting half wedge angle $\omega$ should be taken small enough so that the inclined wedge face does not intersect any of the initially horizontal streamlines. It can be increased gradually after every few time cycles to achieve the desired final angle.

For simplicity, we take the initial values at all mesh points to be uniform as follows:

$$\varrho^0_{l,m} = 1.0,\ v^0_{l,m} = 1.0,\ \beta^0_{l,m} = \tfrac{1}{2}\pi, \quad \text{for} \quad l = 1, 2, ..., L, \quad m = 1, 2, ..., M.$$

The value for initial pressure depends upon the incident shock strength $\xi_I$ and angle $\alpha_I$ specified by the problem. Using oblique shock conditions [7], we have

$$M_I = \{1 + \tfrac{1}{2}[(\gamma - 1)/\gamma](1/\xi_I - 1)\}(\sin \alpha_I)^{-1}, \tag{4.28}$$

and

$$p^0_{l,m} = \varrho^0_{l,m}(v^0_{l,m})^2/M_I{}^2\gamma. \tag{4.29}$$

The choice of $v^0_{l,m} = 1.0$ implies that the initial speed of sound $C_I = 1/M_I$. But $M_I > 1$ if $\xi_I < 1$, from Eq. (4.28). Thus we are guaranteed to have supersonic incoming flow. The desired wedge angle $\omega$ for generating an incident shock with angle $\alpha_I$ can be calculated using the formula [7]

$$\omega = \tan^{-1}\left[2 \cot \alpha_I \frac{M_I{}^2 \sin^2 \alpha_I - 1}{M_I{}^2(\gamma + \cos 2\alpha_I) + 2}\right]. \tag{4.30}$$

Other constants used for all calculations in this work are

$$\gamma = 1.4, \quad \mu = 0.01, \quad L = 50, \quad M = 25,$$
$$\Delta h(\text{space-step}) = 0.05, \quad \text{and} \quad \Delta t(\text{time-step}) = 0.02,$$

where $\Delta t$ has been chosen to satisfy the stability conditions [9]

$$\Delta t \leq (\Delta h)^2 \varrho \eta^2 [\tfrac{16}{3}\mu(\zeta^2 + \eta^2 + 1)]^{-1} \tag{4.31}$$

and

$$\Delta t \leq \tfrac{8}{3}\mu/\gamma p \tag{4.32}$$

The choice of computational constants in the present problem has little effect on the shock-reflection angles. They are chosen to maintain stability of the numerical scheme and to give reasonable computer outputs. For example, the constant $\mu = 0.01$ is obtained by equating the right-hand sides of conditions (4.31) and (4.32).

The main computer program is written in FORTRAN II language with inner iteration loop coded in ILLIAC II machine language. We test for stationary solution of a given shock-reflection problem by comparing all flow variables between every 40 time cycles. If the relative differences are found to be negligible, we stop the computation. The average number of time cycles required for stationary solution is about 600 which takes about 15 minutes of machine time. This includes the time of starting computation from initially uniform flow with an inclined wedge until flow becomes stationary and the time of writing flow data on a magnetic tape.

The method of obtaining incident and reflected shock angles from our computer output is demonstrated in Fig. 3 for the case of $\xi_I = 0.9$, $\alpha_I = 56.0°$, and $\alpha_R = 60.8°$. First we hand-draw constant-density lines on a computer-printed density-variations chart. The various smeared-out shock regions can be seen clearly from the sharp increases of densities in this chart of streamlines. In transplanting the same constant-density lines onto a computer-printed streamline chart in physical space in rectangular coordinates, they become slightly curved. The average of the angles of constant-density curves measured at the reflected-shock region is the desired reflected-shock angle. The beginning of the incident- and the reflected-shock regions are recognized (see lower part of Fig. 3) by staying, say, 5 streamlines away from the wall. This is to avoid the shock-interaction zone arising from the smeared-out effect in our numerical calculation. The loci from which $\alpha_I$ and $\alpha_R$ are measured on each constant density curve are also shown in Fig. 3. The same technique was applied to velocity and pressure variation charts to verify the results.

Some results of this work are shown in Fig. 4. For the incident shock strength $\xi_I = 0.9$, we plot reflected shock angle $\alpha_R$ versus given incident angle $\alpha_I$. (Due to difficulties encountered in displaying computer output, we did not obtain data for $\alpha_I \geq 67°$.) The results obtained by our true viscosity model are in very good agreement with Smith's data. The Rankine–Hugoniot conditions across the reflected shocks are also satisfied with less than 2% error. More numerical data for $\xi_I = 0.8$ and 0.7 can be found in [9]. They too agree well with experimental results. In Fig. 4, we also give results predicted by Von Neumann's [1] theories and numerical results with no explicit viscosity effect, i.e., set $\mu = 0$ in our computation (the shock regions are also smeared out in this case due to the interpolation process—the so-called implicit viscosity effect). (Numerical and experimental data points are fitted by 4th-degree least-square polynomials in the figure for easy comparison.) They do not agree as well in the Mach-reflection region as we can see. This leads us to believe that the true viscosity effect is not negligible for weak Mach-reflection problems. Another feature of the present method is that it gives

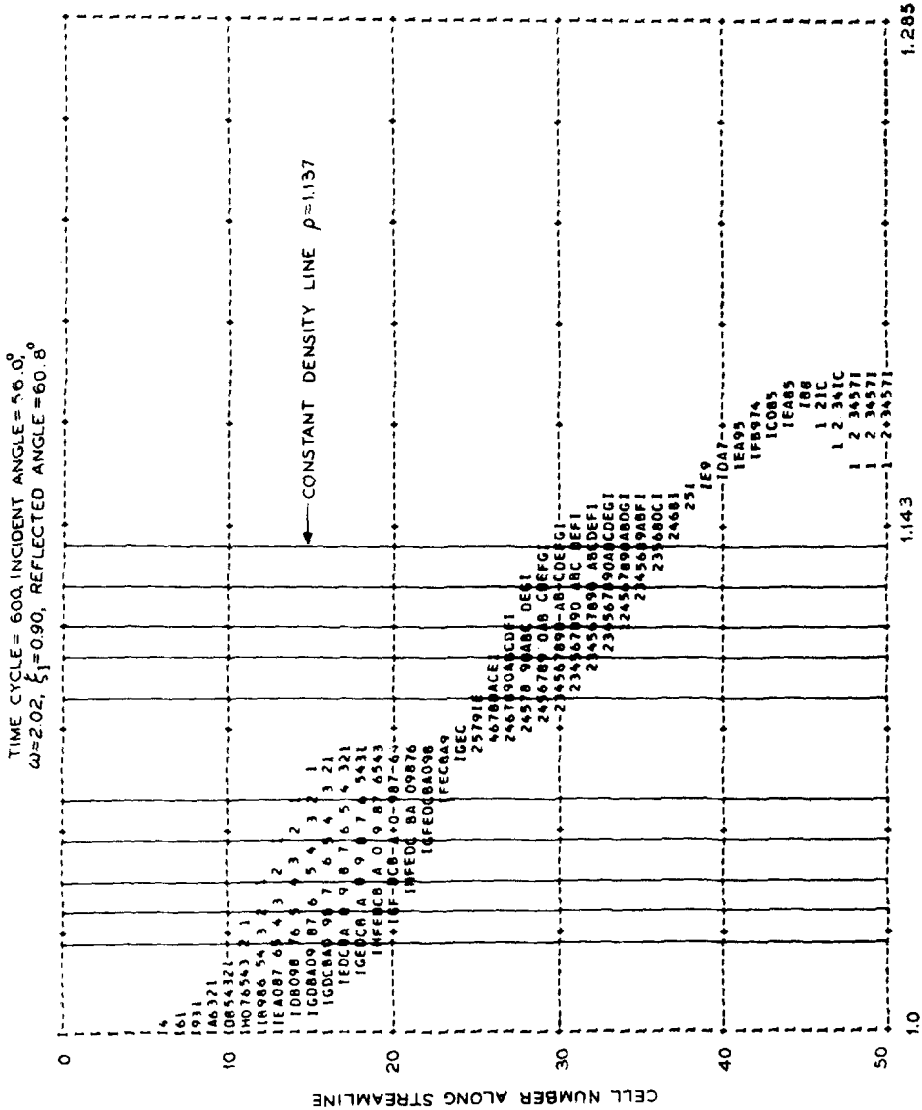
TIME CYCLE= 600, INCIDENT ANGLE=30.0°
ω=2.02, ξ1=0.90, REFLECTED ANGLE=60.8°
CONSTANT DENSITY LINE ρ=1.137
CELL NUMBER ALONG STREAMLINE
DENSITY ρ
1.0
1.143
1.285
0
10
20
30
40
50

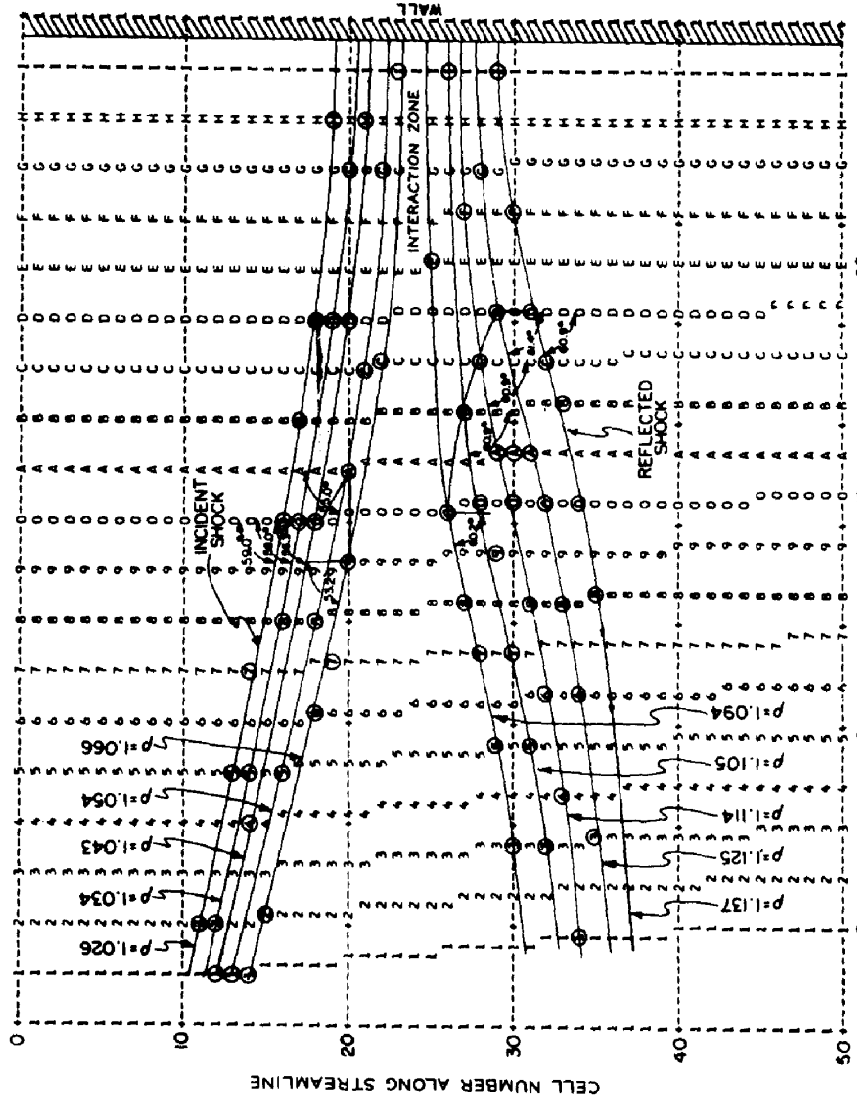


FIG. 3. Measurement of reflected-shock angle from computer output.

a faster technique for numerical solution of shock-reflection problems and it is directly applicable to stationary viscous fluid flow problems.

In this work, we have numerically integrated the time-dependent viscous equations to obtain asymptotically stationary solutions for weak-Mach-reflection

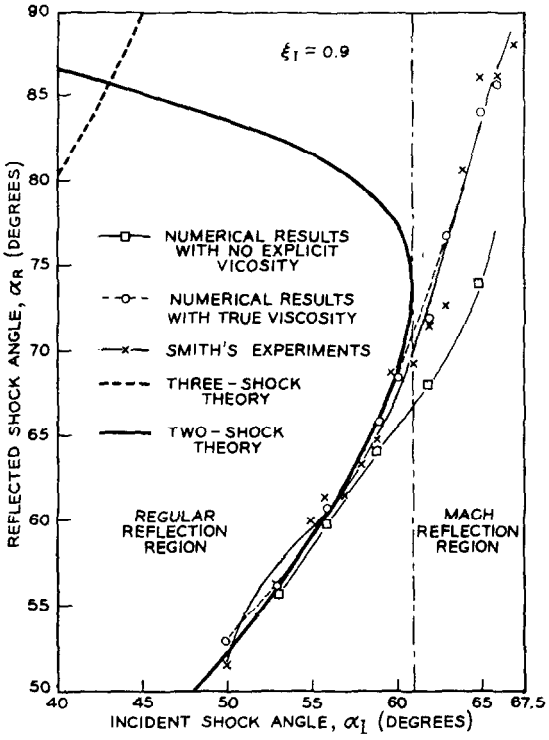


FIG. 4. $\alpha_R$ vs $\alpha_I$ for $\xi_I = 0.9$.

problems. We used streamline-like coordinates to simplify the needed interpolation process and the boundary conditions. The most significant of all, the addition of true viscosity terms in the new coordinates did not complicate the numerical procedure, yet it gives much better results than any other method. Furthermore, we are also the first to analyze the stability of the two-dimensional difference scheme [9]. The stability condition (4.31) gives us the size of time-step when space-step is specified. The only difficulty encountered in the present problem was to choose an appropriate set of computational constants for numerical stability and computer display of results.

There are several ways to improve the efficiency of the present numerical scheme.

For shock-reflection problems, a stationary incident shock could be maintained in the two-dimensional computational region. This is because the generation of incident shocks by placing a wedge in a uniform flow turned out to be quite time-consuming. As for the iteration process itself, the rate of convergence may be increased by using appropriate relaxation schemes. For example, in treating asymptotically stationary problems, the time is no longer physically meaningful because it is used in iteration to avoid numerical difficulties. We can consider variable optimum time-steps at each mesh point instead of a uniform time-step for the whole mesh. This local time-step may serve as a type of relaxation parameter to improve the convergence rate.

ACKNOWLEDGMENT

The author wishes to thank Professor C. W. Gear of the Department of Computer Science, University of Illinois for his guidance in the research and help in the preparation of this work. Valuable comments by the referees are also appreciated.

REFERENCES

1. J. VON NEUMANN, "Oblique Reflection of Shocks," Explosives Research Report No. 12, U.S. Navy Department, Washington, D. C. (1943).
2. L. G. SMITH, "Photographic Investigations of the Reflection of Plane Shocks in Air," Report No. 6271, OSRD, Washington, D. C. (1945).
3. L. CROCCO, "A Suggestion for the Numerical Solution of the Steady Navier–Stokes Equations," Paper No. 65–1 (2nd Aerospace Science Meeting, New York City), American Institute of Aeronautics and Astronautics (1965).
4. S. Z. BURSTEIN, *AIAA J.* **2**, 2111–2117 (1964).
5. F. H. HARLOW, *Proc. Symp. Appl. Math.* **15**, 269–288 (1963).
6. J. VON NEUMANN and R. D. RICHTMEYER, *J. Appl. Phys.* **21**, 232–237 (1950).
7. H. W. LIEPMANN and A. ROSHKO, "Elements of Gasdynamics." Wiley, New York (1957).
8. A. H. TAUB, *Ann. Math.* **62**, 300–325 (1955).
9. T. S. SHAO, "Numerical Solution of Plane Viscous Shock Reflections," Report No. 190, Department of Computer Science, University of Illinois (1965).